Nonlinear Vibrational Response of the Amide I, II, III and A Bands of NMA: Simulation Study Based on an Electrostatic DFT Map

Tomoyuki Hayashi, Wei Zhuang, and Shaul Mukamel
Department of Chemistry, University of California, Irvine, California 92697, USA

Coherent multidimensional infrared spectroscopy provides a valuable tool for protein structure determination[1]. The amide infrared absorption bands originating from stretching and bending of the peptide bonds provide a useful probe for secondary-structure changes because of their sensitivity to hydrogen bonding, dipole-dipole interactions and geometry of the peptide backbone. Most effort has been focused on the Amide I band[2-4] and its cross peaks[5]. However, the cross peak pattern of other amide bands can provide additional structural information. In this paper we simulate the photon-echo signals of the amide I, II, III and A bands in N-methyl acetamide (NMA), which is the simplest model for the amide system.

MD simulations were performed using the CHARMM force field for NMA and TIP3 water at constant temperature (300 K) and volume (NVT) using the CHARMM package. One NMA and 1000 water molecules were held rigid using the SHAPE and SHAKE algorithms respectively.

The fluctuating vibrational Hamiltonian was constructed using an electrostatic model[6,7], which includes the fundamental and overtone frequencies of each of the four amide vibrations, their combination bands, and the transition dipole matrix. The fundamental frequency of each amide vibration is given by $\varepsilon(E) = \varepsilon_{gas} - \delta\varepsilon(E)$ where ε_{gas} is the experimental frequency of an isolated NMA in the gas phase. To calculate the fluctuation $\delta\varepsilon(E)$, we first carried out geometry optimization of an isolated NMA at the BPW91/6-31G(d,p) DFT level using Gaussian03. The middle point of the carbonyl oxygen and the amide Hydrogen of the optimized structure was chosen as a reference point. . A DFT map was constructed which relates $\delta\varepsilon(E)$ to a 19 component vector $\mathbf{C}^T \equiv (E_x, E_y, E_z, E_{xx}, \cdots, E_{xxx}, \cdots)$ representing all independent components of the electric field, its gradients and second derivatives at the reference point:

$$\delta\varepsilon(E) = \mathbf{O}_{\alpha}^{\nu(1)T}\mathbf{C} + \frac{1}{2}\mathbf{C}^T\mathbf{O}^{\nu(2)}\mathbf{C},$$

where $\mathbf{O}^{(1)}$ is a 19 component row vector and $\mathbf{O}^{(2)}$ is a 19x19 matrix, both obtained from the DFT calculations. For each configuration along the 1 fs timestep 1 ns trajectory, three electric field components at 67 points in space which span the transition charge density region of the amide modes [figure 2 in ref5] were calculated. The components of C^T were determined at each time point by a least-square fit to the electric field sampled at these 67 points. C^T calculated using this protocol represents the electric field distribution across the transition charge density region. A similar map was created for the diagonal anharmonicities and transition dipoles.

The resulting map provides the entire fluctuating Hamiltonian required for simulations of third order spectra (fundamental and overtone frequencies as well as the transition dipole magnitudes and directions) from first principles. It has several advantages over other empirical maps which predict the linewidth with comparable accuracy[7,8]. First, it gives a clear physical picture for the origin of the solvent shift of the amide bands; we found that the global sampling of

the spatially nonuniform electrostatic field across the region of transition charge densities (TCDs) of amide modes is essential for the accurate prediction of solvent shifts[5]. Second, the map is not optimized to a particular solvent or solvent environment and is therefore transferable.

The third-order response functions were calculated using the cumulant expansion of Gaussian fluctuations model (CGF) [1]. The photon-echo signal $S(\omega_1, t_2 = 0, \omega_3)$ was obtained by 2-D Fourier transform with respect to the time delays t_1 and t_3 (shown in Fig. 1) by selecting the resonant transitions assuming rectangular frequency pulse shapes with bandwidth of 250 cm^{-1} within the rotating wave approximation. $|S(\omega_1, t_2 = 0, \omega_3)|$ in two frequency regions are displayed in Fig. 2. In the left panel the three incident pulses are tuned to 1500 cm^{-1}. The diagonal and off-diagonal peaks of amide I, II, and III are observed at $(\omega_1, \omega_3) = (-1670,1670), (-1515,1515), (-1293,1293), (-1515,1670), (-1293,1670), (-1293,1515)$. In the right panel where the third pulse is tuned to 3300 cm^{-1}, cross peaks of amide A with amide I, II and III modes are observed at $(\omega_1, \omega_3) = (-1670,3450), (-1515,3450), (-1293,3450)$. The amide A band is hidden underneath the broad O-H stretch band of water, nevertheless its cross-peaks with the amide I, II and III modes can be observed in the photon echo signal. The imaginary part of the diagonal amide I, II and III photon echo peaks and their cross peaks are displayed in Fig. 3. The elliptical elongated peak shapes indicate that the broadening is inhomogeneous. The negative and positive peaks along ω_3 come from stimulated emission and ground state bleach respectively. Anharmonic shifts of amide I, II and III defined as the frequency differences between the two peaks are 17 cm^{-1}, 13 cm^{-1} and 13 cm^{-1} respectively. The calculated diagonal and off-diagonal anharmonicities of amide modes of NMA in water are listed in Table. 1. The anharmonic shifts of amide I and III are larger than these anharmonicities due to interference between the two peaks. Only the amide I and II cross peak shows a positive peak at larger ω_3 due to its negative anharmonicity. The simulated linewidths of the amide I, III and A bands are in good agreement with experiment. The amide II liewidth is underestimated. One possible reason is that its highly delocalized transition charge density extends over regions of the amide and methyl groups which are not sampled in the present simulations.

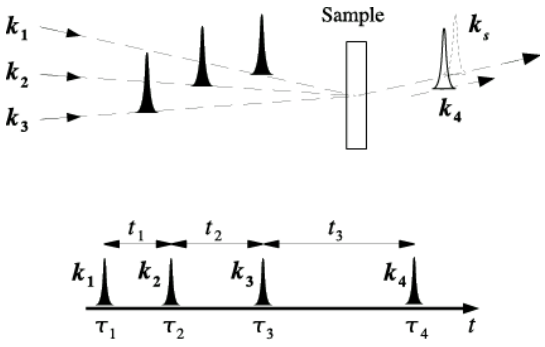

Fig. 1 Laser pulse sequence (upper panel), the peak ordering and time variables (lower panel) in the photon echo experiment. $\mathbf{k}_s = -\mathbf{k}_1 + \mathbf{k}_2 + \mathbf{k}_3$.

Table 1. Diagonal and off-diagonal anharmonicities (in cm^{-1})

	I	II	III
I	14.3	−3.1	19.7
II		13.0	11.0
III			10.7

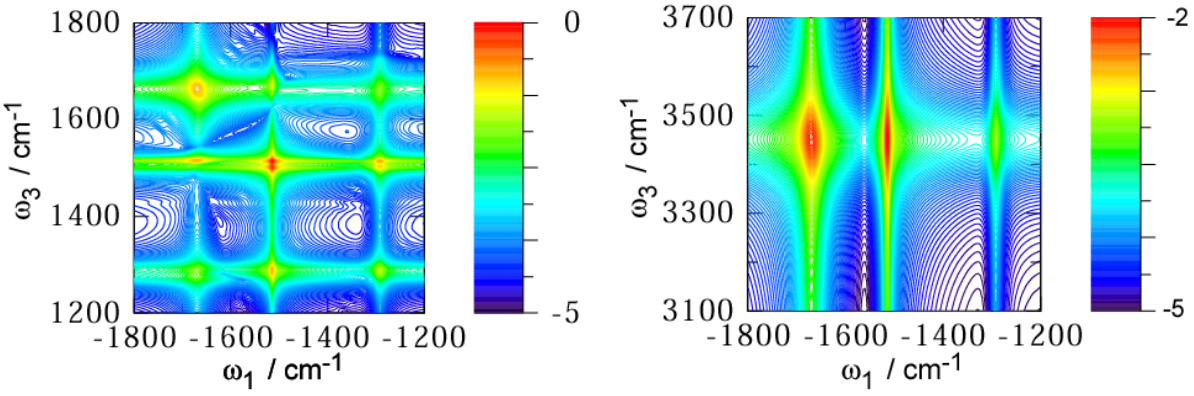

Fig. 2: Photon echo signals $\log|S(\omega_1, t_2 = 0, \omega_3)|$ of NMA. Left: The amide I, II, III frequency region; right: cross peaks between amide A (ω_3) and amide I, II, III(ω_1)

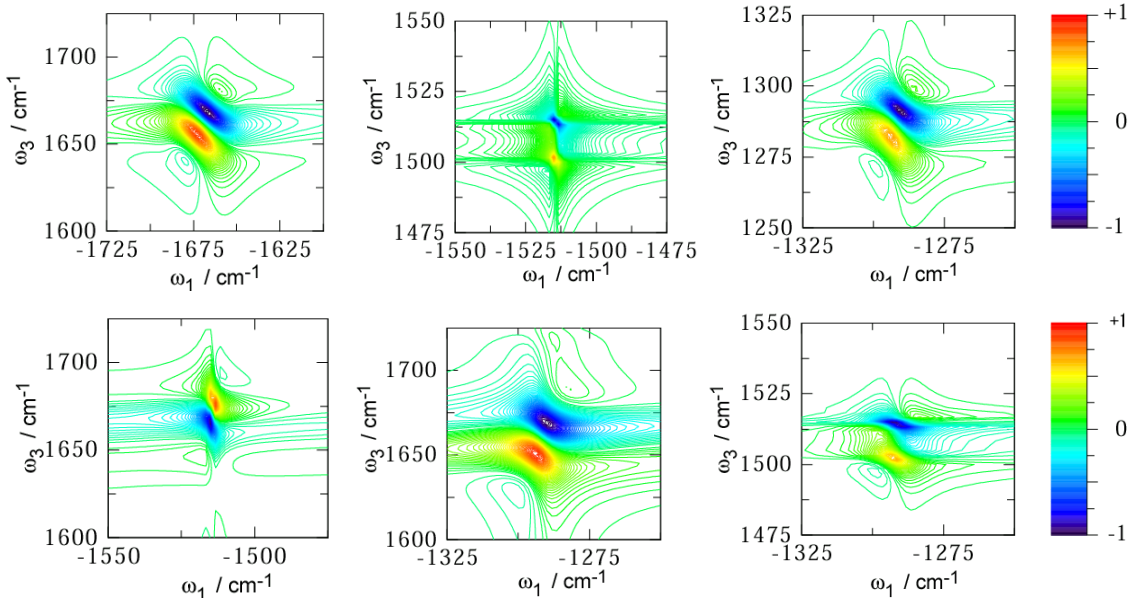

Fig. 3: Photon echo spectra $\mathrm{Im}[S(\omega_1, t_2 = 0, \omega_3)]$. Top: Diagonal peaks; amide I (left), II (center), III (right). Bottom: cross peaks; I-II (left), I-III (center), II-III (right).

The support of the National Institutes of Health grant no. (RO1GM59230-04) and the National Science Foundation grant no. (CHE-0446555) is gratefully acknowledged.

1. D. Abramavicius and S. Mukamel, *Chem. Rev.* **104**, 2073 (2004)
2. P. Hamm, M. Lim, W. F. DeGrado, and R. M. Hochstrasser, *PNAS,* **96**, 2036 (1999)
3. A. Moran, S. -M. Park, J. Dreyer, and S. Mukamel, *J. Chem. Phys.* **118**, 3651 (2003)
4. M. F. DeCamp, L. DeFlores, J. M. McCracken, A. Tokmakoff, K. Kwac, M. Cho, *J. Phys. Chem. B* **109**, 11016 (2005)
5. I. V. Rubtsov, K. Kumar, R. M. hochstrasser, *Chem. Phys. Lett.* **402**, 439 (2005)
6. T. Hayashi, W. Zhuang, and S. Mukamel, *J. Phys. Chem. A* (in press) "Electrostatic DFT Map for the Complete Vibrational Amide Band of NMA"
7. T. Hayashi, T. l. Jansen, W. Zhuang, and S. Mukamel, *J. Phys. Chem. A* **109**, 64 (2005)
8. S. A. Corcelli, C. P. Lawrence, and J. L. Skinner, *J. Chem. Phys.* **120**, 8107 (2004)